buildings

MDPI

*Article*

# Optimization of Composition of Waterproofing Material Based on Modified Fine-Grained Concrete

**Aleksey Zhukov, Sofia Bazhenova, Irina Stepina * and Irina Erofeeva**

Department of Building Materials Science, National Research Moscow State University of Civil Engineering, 129337 Moscow, Russia; lj211@yandex.ru (A.Z.); sofia.bazhenova@gmail.com (S.B.); ira.erofeeva.90@mail.ru (I.E.)
* Correspondence: sudeykina@mail.ru

**Abstract:** The purpose of the research described in this article was to optimize the compositions based on hydraulic-modified binder and construction waste for waterproofing and repair of concrete or brick structures in contact with the ground, as well as the study of properties and development of the basis of the methodology for selecting the composition of such a waterproofing system. Processing of the results of the experiment was carried out by statistical and analytical methods. The research was based on a method for determining the adhesive strength of a waterproofing coating, based on the determination when the insulating layers are torn off. As a result of the calculation and experimental verification, the composition of the waterproofing material was obtained, which corresponds to an adhesive strength of 3.8 MPa; the strength of the waterproofing layer was 36–37 MPa, as well as the amounts of the main components: acrylic resin 3.9%; finely ground concrete waste 80 kg/m$^3$; plasticizer consumption (0.38. . .0.39%) at the optimum moisture content of the base surface (9.7. . .9.8%).

**Keywords:** modified concrete; waterproofing; hydraulic binder; acrylic resin; plasticizer; construction waste; adhesive strength; compressive strength



**Citation:** Zhukov, A.; Bazhenova, S.; Stepina, I.; Erofeeva, I. Optimization of Composition of Waterproofing Material Based on Modified Fine-Grained Concrete. *Buildings* **2024**, *14*, 1748. https://doi.org/10.3390/buildings14061748

Academic Editor: Xiaoyong Wang

Received: 6 May 2024
Revised: 23 May 2024
Accepted: 7 June 2024
Published: 10 June 2024



## 1. Introduction

Waterproofing can be considered as a building system that provides protection of the structure from vapor–air mixtures and drip moisture (molar and molecular moisture transfer). The components of the waterproofing system are a base material (usually heavy concrete or reinforced concrete) with reduced water permeability, waterproofing membranes, protection of waterproofing membranes, drainage systems, and thermal insulation. All these materials and technologies for their application are components of the waterproofing subsystems of individual parts of the building and structures that are in contact with environmental moisture or ground moisture [1–3].

Firstly, there are flat and pitched roof insulation subsystems. Secondly, there are the systems of insulation of facades and the basement of buildings. Thirdly, there are insulation systems for structural elements of a building that are in contact with the ground, i.e., the foundations, basements, and floors on the ground. Fourthly, there are insulation systems for tunnels and other underground structures. Each of the waterproofing subsystems has features in terms of the materials used, design solutions, and methods for implementing these solutions [4–6]. 'General' is the declared main purpose of these systems.

In addition to direct waterproofing, each of the subsystems assumes the presence of a structurally designed drainage system, usually with the use of engineering structures or mechanisms. The impact of water (drop liquid with mineral and, in some cases, organic substances dissolved in it) is one of the main factors affecting the durability of structures. Water, filtering through the waterproofing system, penetrates into structures and initiates corrosion processes in the materials that form these structures. Corrosion leads to the degradation of the properties of the structure and its subsequent destruction. First of all,

the insulation systems (if they are provided for by the project) and reinforced concrete of the base are exposed to corrosion [7–9].

To the greatest extent, the manifestation of negative consequences in the protection systems "drip moisture-construction" takes place for structures partially or completely buried in the ground. On the one hand, the chemical composition of moisture and its ability to penetrate through the smallest leaks and crevices, as well as the factor of hydrostatic (and in the case of running water, hydrodynamic) pressure negatively affect the properties and durability of structures [10–12]. On the other hand, the buried structures themselves have an impact on the properties of the surrounding soils and groundwater. Firstly, there is a draining effect that buried structures have on the groundwater level. The mechanism here is as follows: water seeps into tunnels or pits, it is pumped out with the help of pumps, while the level of moisture in the soil and its water saturation can change, which leads to a change in the properties of the soil, the chemical composition of groundwater, which can affect both the quality of construction work, and the durability of the insulation system [13–15].

Practice shows that water leakage into a tunnel during the construction phase can cause changes in hydrogeology with an increase in groundwater flow and a decrease in groundwater levels in bedrock and overburden, which leads to a change in hydrochemistry. Also, the state and chemical composition of groundwater can be influenced by the chemical composition of the applied waterproofing solutions, as well as solutions used to strengthen the soil [16–18].

The processes of degradation of the properties of waterlogged structures can be intensified due to the additional influence of external factors. These are wind and vibration loads, and sign-variable temperatures, and the impact of biological aggressors of various nature. As a result of moistening, such problems appear as corrosion of concrete, reinforced concrete, and metal structures of buildings; corrosion of embedded parts and fittings; freezing of enclosing elements; biodamage; as well as direct flooding of objects is possible.

Roof systems experience mainly the effects of rain, snow, the possibility of frost formation, and, as a concomitant effect, wind loads. On pitched roofs, external drainage is assumed. The waterproofing carpet is made solid, as a rule, along a continuous crate with reinforcement in problem areas and, on skates, junctions of multi-level roof elements, as well as in valleys, and along the perimeter of passage elements, i.e., pipes, aerators, wind vanes, antennas, etc. On flat roofs and roofs, as a rule, internal drains are provided through receiving funnels [19–21]. In inverted exploited roofs with intensive or extensive landscaping, such funnels are two-level. Moisture is removed both from the surface of the roof and from the inner layers of the roof structure. In this case, a profiled membrane with a geotextile coating is used [22–24].

The impact of wind loads can lead to negative results for a roof of any kind and any configuration. These loads are especially intense at high wind speeds, such as typhoons, tornadoes, and gust winds. The air flow penetrates under the outer protective and decorative layer and tears off both the waterproofing and other layers that form the roofing pie of the structure. As a rule, destruction occurs due to failure of the mechanical fastening of waterproofing membranes [25–27].

Facade waterproofing systems are usually based on the use of multi-layer plaster systems that perform both protective and decorative functions. In the case of using systems with insulation, the design solutions for facade insulation become more complicated and significant. In this case, it is necessary to implement additional structural measures to protect the heat-insulating materials that form the insulating shell. From the side of the room, the use of a vapor barrier or diffuse membranes is recommended; from the outside—waterproofing [28–30]. In the basement of the building, cut-offs made of rolled insulation are required to prevent capillary suction of moisture from the foundation in the wall structure (Figure 1).

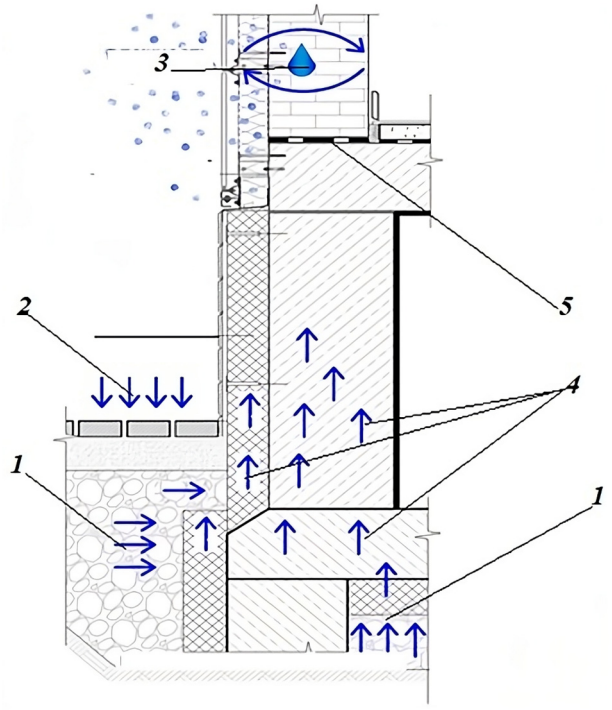


**Figure 1.** Methods of moisture penetration into the structure: 1—ground moisture; 2—precipitation (snow, rain) and melt-water; 3—air humidity; 4—moisture filtration due to capillary phenomena; 5—waterproofing cut-off.

Moisture can get into structures in various ways (see Figure 1). In the construction of the wall, of its basement, and foundation, there is a constant movement of the vapor–air mixture. With the possibility of moisture condensation under certain conditions, for example, when the material reaches the dew point temperature. If the insulation system is not properly implemented, capillary rise of ground moisture through the foundation structure and through the capillaries of the wall material is possible.

For insulation systems of any structures in contact with the ground (foundations, operated basements, tunnels, etc.), four aspects are important: reducing the water permeability of the supporting structure, creating seamless insulating shells, protecting the insulation system from external physical and physico-chemical impacts and an efficient drainage system (Figure 2).

The bearing structures of underground structures are usually made of heavy concrete (reinforced concrete) with a water permeability rating of at least W8. If the structure is made of separate elements (shells), sealing of the joints is mandatory. If the water resistance is insufficient, then it is possible to strengthen the structures by injecting special polymer or polymer–cement solutions into them. If it is necessary to insulate (for example, the walls of an operated basement), heat-insulating boards are used that not only have good strength characteristics, but also have low water absorption, water resistance, and are also resistant to aggressive groundwater, e.g., boards based on extruded polystyrene foam (XPS -plates), or polyisocyanurate foam (PIR-plates) [31–33].

For all their advantages, constructions made of slab heat-insulating products have a significant drawback: the presence of leaks on the contact surfaces between the slabs and between the slabs and supporting structures. These areas of increased heat transfer, called “cold bridges”, significantly reduce the thermal performance of the structure. In this regard, seamless insulating shells are considered promising, which are used not only for insulating structures in contact with the ground, but also for insulating walls and the foundations of structures and roofs [34,35]. Firstly, there are heat–vapor-waterproofing shells based on polyurethane foam or polyethylene foam. Secondly, there are light or warm plaster coatings (used mainly for wall insulation), as well as green walls. Thirdly, there are

polymer concretes and modified concretes based on a hydraulic binder, used mainly for the insulation of underground structures [36–39].

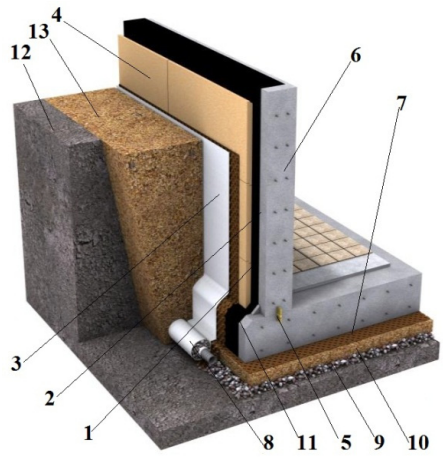


**Figure 2.** The system of heat–hydro–vapor barrier for the insulation of the operated basement: 1—waterproofing roll material; 2—bituminous primer; 3—profiled membrane PLANTER geo; 4—plates made of extruded polystyrene foam (XPS) or polyisocyanurate foam (PIR), or hekjys made of seamless polyethylene foam (PE); 5—PVC waterstop, central; 6—foundation wall; 7—profiled membrane PLANTER standard; 8—drainage pipe; 9—crushed stone preparation; 10—sand preparation; 11—transitional side (fillet); 12—base soil; 13—backfill soil.

Polymer concretes and fine-grained modified concretes used in underground insulation systems have several advantages over other materials. Firstly, the introduction of polymer components into the composition makes it possible to obtain materials with a water resistance grade of W10 and higher. Secondly, the components of such concretes and the hydraulic binder have a high degree of affinity with the base material, which, as a rule, is concrete. The strength of the contact is thus ensured at the physicochemical and chemical levels due to reactions in the contact, or rather in the transition zone. Thirdly, as part of waterproofing fine-grained concrete, it is possible to use recycled concrete waste, which expands the attractiveness of using the material from the standpoint of waste disposal and solving environmental problems [40,41].

An effective way to protect the concrete of underground structures from moisture and damage by aqueous solutions containing aggressive chemicals is the hydrophobization of the surface of structural concrete (reinforced concrete), as well as the use of fine-grained, polymer-modified concrete based on a hydraulic binder.

Waterproofing materials based on a hydraulic binder have high adhesion to the base material (usually concrete or reinforced concrete), which is explained by the same crystal structure; the same mechanism for the formation of a strong shell, which is based on the hydration processes of clinker minerals; as well as close physical properties (including the coefficient of thermal expansion) with concrete and high compressive strength.

Thus, the waterproofing coating must meet the following requirements: to ensure maximum watertightness in any, even the most critical, operating conditions, as well as to form a strong contact with the base material. These conditions correspond to the waterproofing systems based on mineral-modified binders, especially since, with the help of these systems, it is possible to create seamless waterproofing shells, and in the composition of the binder, it is possible to partially utilize treated construction waste.

Two systems are most commonly used in waterproofing methods; those with a waterproofing barrier (made of roll material or membranes) and those based on plaster systems containing hydraulic binder. Such systems were studied in the experiment.

Coating efficiency was assessed by the following criteria: the condition of the coating surface; the intensity of corrosion processes in the surface layer and in the coating body,

including the contact surfaces of the base material and the coating; as well as the adhesion of the coating to the substrate.

The condition of the surface and surface layers of concrete was assessed using appropriate instruments or non-destructive methods, as well as visually. A thorough inspection of the concrete surface was carried out. The presence of shells, abrasions, delaminations, wear, and other defects were recorded, and the depth of corrosion damage in the surface layers of concrete (reinforced concrete) was also assessed.

Determination of the depth of concrete corrosion damage and the state of reinforcement was carried out either by non-destructive methods, including using electron tomography, or on the basis of determining the depth of concrete neutralization (changes in its alkalinity in the surface layer due to reactions with air $CO_2$). The colorimetric method is the least expensive and most obvious way to determine the depth of neutralization.

The colorimetric method consisted of the following. The cores drilled out of the concrete body were split and the freshly formed surface of the chip was wetted with a 0.1% alcohol solution of phenolphthalein. Crimson coloration of the surface of the concrete wetted with a solution was manifested at a pH of more than 8.3, which allowed us to conclude if there was an acidic environment (formed during carbonate corrosion and leaching of concrete). The original color of the surface was maintained at a pH of less than 8.3.

Depending on the type of structure and the conditions of its operation, as well as the time of operation, the depth of concrete neutralization varied from 2–4 mm to 20–50 mm, and in some months (under the influence of an additional alternating temperature effect—up to 100 mm. According to the results of chemical analysis, it is possible to draw a conclusion about the state of concrete of underground structures. Practice shows that concrete in contact with running water is exposed to the greatest leaching effect. In such cases, corrosion of the first and second type prevails.

The purpose of the research described in the article was to optimize the compositions based on hydraulic-modified binder and construction waste for waterproofing and repair of concrete or brick structures in contact with the ground, as well as the study of properties and the development of the basis for the methodology for the selection of the composition of such waterproofing systems.

## 2. Materials and Methods

Portland cement (activity 40 MPa) and finely ground waste, the specific surface of which was comparable to the specific surface of Portland cement: 300–350 $m^2/kg$, were used in the composition of waterproofing systems. Particles with a shape close to spherical predominated. Acrylic resin produced in Russia at the Bobrovsky experimental plant was used as an acrylic additive.

Evaluation of coating strength properties and adhesion of the coating to the substrate were the main instrumental methods to determine the quality characteristics of the coating.

Tensile adhesion tests were carried out using the DYNA instrument. With the help of drilling perpendicular to the insulated surface, an incomplete (partial) sample with a diameter of 50 mm was taken. The core (sample) passed through the interface (between the waterproofing material and concrete) deeper into the concrete base. A metal disk was attached to the surface of the core using epoxy resin, and after it had cured, a pull-off force was applied to this disk (Figure 3).

The load was applied at a constant rate until the moment of destruction. Tensile strength was determined as the ratio of the value of the fixed breaking load to the cross-sectional area of the cylindrical sample. At the same time, the type of destruction and the place where the destruction occurred were taken into account, i.e., along the concrete, along the contact zone (interface), or along the waterproofing layer. As an indicator of adhesive strength, only the destruction that occurred at the interface between materials was taken. Destruction in the concrete or a waterproofing (repair) layer was considered as the lower limit estimates of adhesive strength.

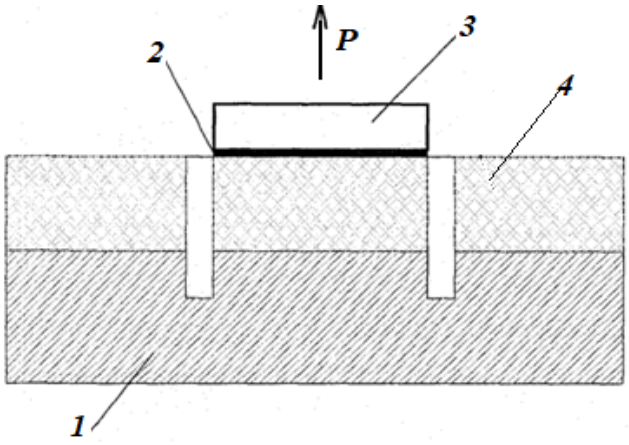


**Figure 3.** Pull test scheme: 1—base concrete (bearing structure); 2—polyepoxy glue; 3—metal disk; 4—waterproofing (repair) material; P is the direction of tension (application of the load generated by the test device).

In the experiment, for the conditions which are presented in Table 1, the influence on the adhesion strength ($Y_1$) and on the compressive strength of modified waterproofing fine-grained concrete ($Y_2$) of four factors was studied: the consumption of acrylic additive in a mineral waterproofing material based on hydraulic binder ($X_1$), the moisture content of the base surface ($X_2$), as well as the consumption finely ground concrete waste ($X_3$) and plasticizer consumption ($X_4$). The optimization parameter was taken to be the adhesion strength ($Y_1$) of the waterproofing coating to the base material.

**Table 1.** The adhesion strength (Y1) and on the compressive strength of modified waterproofing fine-grained concrete

| Factor Name | Mathematical Symbol | Average Value | Variation Interval | Values on Levels | |
|---|---|---|---|---|---|
| | | | | −1 | +1 |
| The consumption of the polymer component (acrylic addition), $P_{pc}$, % | $X_1$ | 2.4 | 1.6 | 0.8 | 4.0 |
| Surface humidity, w, % | $X_2$ | 6 | 4 | 2 | 10 |
| Consumption of finely ground concrete waste, $P_{cw}$, kg/m$^3$ | $X_3$ | 80 | 40 | 40 | 120 |
| Plasticizer consumption, $P_p$, % | $X_4$ | 0.28 | 0.12 | 0.14 | 0.40 |

The consumption of Portland cement (grade M400) was assumed to be 280 kg/m$^3$; the consumption of fine aggregate (quartz sand with fineness modulus Mk 2.3) was 360 kg/m$^3$. The flow rate was assigned depending on the required workability of the concrete mixture and was carried out by the standard method. The waterproofing material was applied to the samples, and then, after 28 days, their adhesion strength in tension and separately for the strength of the surface layer in compression were tested according to the standard test method.

The experiment was conducted using a four-factor experiment matrix based on a D-optimal plan. At each point of the plan, the experiments were carried out at least five times. To reduce the possible influence of extraneous factors, the sequence of experiments was randomized. The "scatter" of the results for each series of experiments was evaluated using the Cochran criterion.

The adequacy of the obtained models was checked using Fisher's criterion. This criterion is based on the determination of the calculated values of the F-criterion and its comparison with the tabulated values calculated for degrees of freedom f1 = 4 and degree of freedom f2 equal to the number of free coefficients in each of the regression

equations. When determining the calculated values of the F-criterion, the sum of squares of the difference between the calculated and average experimental values for each of the experiments was taken into account.

## 3. Results and Discussion

Processing the results of the experiment, carried out in the Statistica program, made it possible to obtain a model (an algebraic polynomial or a function of four variables) that relates the adhesive strength and compressive strength of a waterproofing material with the factors varied in the experiment. The significance of the coefficients of the base polynomials was estimated by confidence intervals ($\Delta b$), which were calculated using the Student's *t*-test. The adequacy of the obtained models was verified by the Fisher criterion. As a result, the following basic mathematical models were obtained:

- For adhesive strength ($\Delta b_1$ = 0.11 MPa):

$$Y_1 = 2.51 + 1.08X_1 + 0.30X_2 - 0.18X_3 - 0.16{X_2}^2 \quad (1)$$

- For compressive strength ($\Delta b_2$ = 0.6 MPa):

$$Y_2 = 32.4 + 3.2X_1 + 1.0X_2 + 1.8X_3 + 1.4X_4 + 1.2X_1X_3 - 0.8{X_4}^2 \quad (2)$$

Adhesion strength, according to the analysis of the coefficients of the model (1), was most determined by the consumption of acrylic resin (coefficient at $X_1$ equal to 1.08); the consumption of finely ground concrete waste affected the adhesive strength but not significantly (the coefficient at $X_3$ was equal to minus 0.18). The influence of base humidity was ambiguous at low and medium humidity values, the adhesive strength increased, but at values exceeding a certain average level, the adhesion strength began to decrease (coefficient at $X_2$ equal to 0.3 and at ${X_2}^2$ equal to minus 0.16). The inflection point of the function $Y_1(X_1, X_2, X_3)$ was within the range of the factor $X_2$, provided by the conditions of the experiment, and the optimal value could be determined analytically.

The compressive strength of the waterproofing coating also depended to the greatest extent on the consumption of acrylic resin (factor at $X_1$ equal to 3.2). To a lesser extent, the compressive strength depended on the surface moisture, the consumption of fine-grained concrete waste (the coefficient at $X_2$ and $X_3$ was equal to 1.0 and 1.8 respectively). When the values of the plasticizer consumption were below the average, provided for by the experimental conditions (the coefficient at $X_4$ was equal to 1.4 and at ${X_4}^2$ was equal to minus 0.8). The inflection point of the function $Y_2(X_1, X_2, X_3, X_4)$ was within the range of the factor $X_4$, provided for in the experimental conditions, and the optimal value could be determined analytically.

The use of the analytical optimization method makes it possible, as a result of the analysis of polynomials obtained by statistical methods, to obtain additional information about the influence of factors (within their variation intervals established by the experimental conditions, Table 1) on the results and obtain optimized response functions. The basis of the methodology is the assumption that the obtained statistical relationships (mathematical models) are algebraic functions of several variables, and methods of mathematical analyses are applicable to these functions [41–43].

Analytical optimization was carried out in five stages: the basic models were first optimized by the surface moisture factor ($X_2$), and then optimized by the plasticizer consumption ($X_2$); the natural values of the optimized factors were determined; a graphical interpretation of the obtained optimized models was carried out; a nomogram was formed for solving inverse and direct problems of mathematical modeling.

Stage 1. Optimization of the obtained basic models for $X_2$: the optimal value of the factor $X_2$ was determined (in coded form), and then both basic Equations (1) and (2) were solved at optimal values of $X_2$.

$$\partial Y_1/\partial X_2 = 0.3 - 3.2X_2 = 0 \rightarrow X_2 \frac{0.3}{0.32} = 0.94$$

Obtaining algebraic polynomials optimized with respect to $X_2$:

- For adhesive strength:

$$Y_1 = 2.65 + 1.08X_1 - 0.18X_3 \quad (3)$$

- For compressive strength:

$$Y_2 = 33.3 + 3.2X_1 + 1.8X_3 + 1.4X_4 + 1.2X_1X_3 - 0.8{X_4}^2 \quad (4)$$

Stage 2. Optimization of model (4) by $X_4$ (model (3) does not contain factor $X_4$): the optimal value of factor $X_2$ is determined (in coded and natural form), and then Equation (4) is solved at optimal values of $X_4$.

$$\partial Y_1/\partial X_4 = 1.4 - 1.6X_4 = 0 \rightarrow X_4 \frac{1.4}{1.6} = 0.875$$

Obtaining algebraic polynomials optimized for $X_2$ and $X_4$:

- For adhesive strength:

$$Y_1 = 2.65 + 1.08X_1 - 0.18X_3 \quad (5)$$

- For compressive strength:

$$Y_2 = 33.9 + 3.2X_1 + 1.8X_3 + 1.2X_1X_3 \quad (6)$$

Stage 3. The determination of the natural values of the optimized factors was carried out using the data presented in Table 1:

Surface humidity: w = 6 + 0.94 × 4 = 9.7. . .9.8%

Plasticizer consumption: Pp = 0.28 + 0.875 × 0.12 = 0.38. . .0.39%

Stage 4. Graphical interpretation of the optimized functions (5) and (6) is shown in Figures 4 and 5.

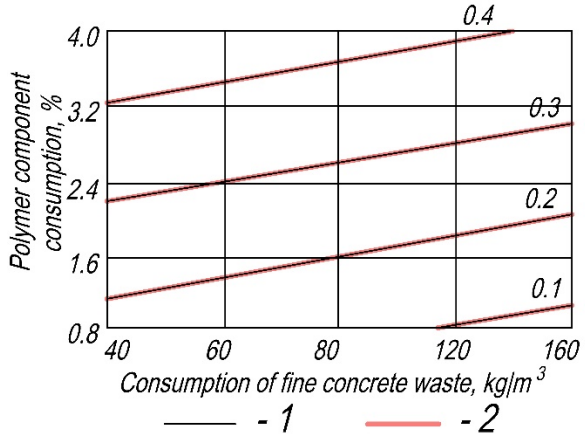


**Figure 4.** Relationship between adhesive strength (MPa) and variable factors at optimal values of surface moisture 9.7. . .9.8% and plasticizer consumption 0.38. . .0.39%: 1—average value; 2—result variance.

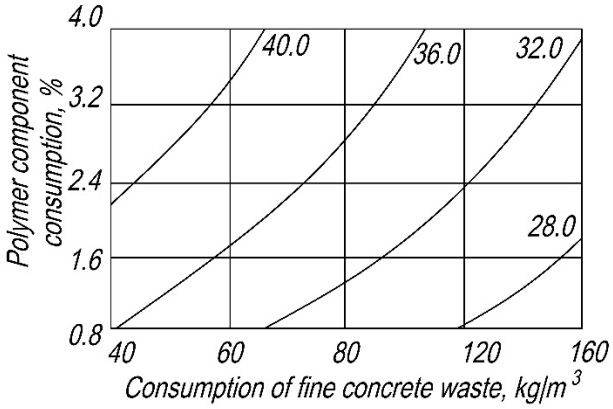


**Figure 5.** Relationship between the strength of the waterproofing layer (MPa) and variable factors at optimal values of surface moisture 9.7. . .9.8% and plasticizer consumption 0.38. . .0.39%.

The uncertainty factor on predicting the results using the optimized functions was accounted for in Figure 4 by introducing the mean value and variance of the result with an accuracy probability of 98%.

It should be noted that the use of analytical optimization allows not only to obtain the values of factors in intervals, including optimal values, but also to reduce the cumbersomeness of graphical interpretation of the obtained results, which can be performed in Cartesian coordinates on the plane in the form of functional dependencies $U = f_1(X_1, X_3)$, or as an equation with a parameter: $X1 = f_2(X_3, U)$.

Stage 5. A nomogram was built for selecting the composition of a waterproofing (repair) material and solving a prognostic problem of mathematical modeling: predicting the properties of this material (Figure 6). The nomogram was constructed by combining the graphical interpretation of the optimized models (5) and (6).

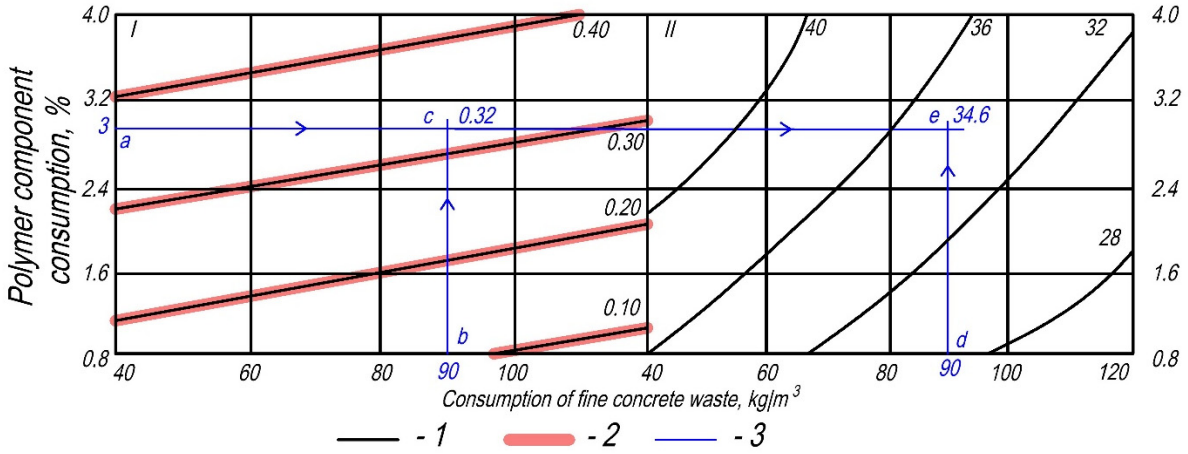


**Figure 6.** Nomogram for selecting the composition and predicting the adhesive strength (MPa) and the strength of the waterproofing layer (MPa) on variable factors at optimal values of surface moisture 9.7. . .9.8% and plasticizer consumption 0.38. . .0.39%: 1—average value; 2—variance of the result; 3—an example of solving a prognostic problem.

The nomogram combines two sectors. In sector I, a problem is solved related to the evaluation of adhesion strength values depending on variable factors; in sector II—the task of assessing the strength of waterproofing fine-grained modified concrete depending on various factors. An example of solving a prognostic problem (estimating the properties of a waterproofing coating depending on the values of variable factors) is shown by orange lines (3) in Figure 6.

The procedure for solving the prognostic problem is as follows. The experimenter sets the values of the consumption factors of acrylate resin and the consumption of finely ground concrete waste. Let the consumption of acrylic resin be 3%; we marked the point "a" on the ordinate axis and drew a straight line (a, e) parallel to the abscissa axis through sectors I and II. We set the consumption of finely ground concrete waste 90 kg/m$^3$. In sector I, from the point "b", we raised the perpendicular to the intersection with the straight line (a, e) and at the intersection we achieved the point "c", which corresponded to an adhesive strength of 0.32 MPa. In sector II, from the point "d" we raised the perpendicular to the intersection with the straight line (a, e) and at the intersection we achieved the point "e", which corresponded to a compressive strength of 34.6 MPa. Optimal values of surface moisture (9.7. . .9.8%) and plasticizer consumption (0.38. . .0.39%) were previously determined as a result of analytical optimization.

After determining the values of the factors using calculation methods, a control series of active experiments was carried out and the actual values of the adhesive strength and compressive strength of the waterproofing coating samples were determined at previously specified values of the variable factors (Table 2). They established the difference between the calculated and natural values and made the final conclusion on the efficiency of the obtained models, as well as on the values of variable factors.

**Table 2.** Verification of the reliability of the results obtained at optimal values of surface moisture 9.7. . .9.8% and plasticizer consumption 0.38. . .0.39%.

| № | Factor Values: | | Adhesion Strength, MPa | | | Compressive Strength, MPa | | |
|---|---|---|---|---|---|---|---|---|
| | Acrylic Consumption, % | Consumption of Finely Ground Waste, kg/m$^3$ | Estimated | Practical | Δ, % | Estimated | Practical | Δ,% |
| 1 | 3.9 | 110 | 3.6 | 3.5 | 2.8 | 39.1 | 37.4 | 4.3 |
| 2 | 3.9 | 80 | 3.7 | 3.8 | 2.7 | 37.1 | 36.1 | 2.7 |
| 3 | 3.9 | 50 | 3.9 | 3.8 | 2.6 | 34.1 | 35.8 | 5.0 |
| 4 | 2.4 | 110 | 2.5 | 2.4 | 4.0 | 35.7 | 34.2 | 4.2 |
| 5 | 2.4 | 80 | 2.7 | 2.5 | 7.4 | 33.9 | 34.9 | 4.3 |
| 6 | 2.4 | 50 | 2.7 | 2.5 | 7.4 | 32.1 | 33.8 | 5.3 |
| 7 | 0.9 | 110 | 1.4 | 1.5 | 7.1 | 31.5 | 30.0 | 5.0 |
| 8 | 0.9 | 80 | 1.9 | 1.8 | 5.2 | 30.7 | 30.0 | 2.3 |
| 9 | 0.9 | 50 | 1.8 | 1.7 | 5.6 | 28.7 | 30.0 | 4.5 |
| | | | Mean deviation: | | 5.0 | Mean deviation: | | 4.2 |

In Table 2, Δ is calculated by the formula: $\Delta = \left|\frac{Y - R_{exp}}{Y}\right| \times 100$

where Y is the estimated value, and Rexp is the experimental value of the parameter.

The optimization parameter is the adhesive strength of the waterproofing coating to the base material. Therefore, according to the magnitude of the results, we took compositions 2 and 3 as the basis of the waterproofing material. The difference between the calculated and experimental values of the adhesive strength varied from 2.8 to 7.4% (average 5.0%), and the compressive strength from 2.3 to 5.3% (average 4.5%). The obtained value of the deviation of the experimental values from the calculated indicators below those accepted in the technology of concrete. In connection with these, the results of the experiment carried out can be considered satisfactory.

Taking into account the percentage of deviations, we accepted 2 as the main composition. This composition corresponded to an adhesive strength of 3.8 MPa; the strength of the waterproofing layer was 36–37 MPa, and the amounts of the main components: acrylic resin 3.9%; finely ground concrete waste 80 kg/m$^3$; plasticizer consumption (0.38. . .0.39%) at the optimum moisture content of the base surface of 9.7. . .9.8%.

The roughness and fracturing of the base surface were important for increasing the adhesive strength, but these parameters are difficult to use as variable factors, since it is practically impossible to comply with the conditions for the continuity of the values of the variable factors over the entire area of their measurement (from −1 to +1) and their reproducibility (measurement method).

The area of contact between waterproofing fine-grained modified concrete and base concrete is considered as a transition zone (transition layer) and the processes occurring in this zone largely determine the magnitude of the contact strength and durability of this contact.

The presence of an optimum function of adhesive strength is explained by chemical and physicochemical processes occurring in the transition layer, including the absorption of moisture contained in the waterproofing material. Moisture is removed from the volume in which the hydration of the hydraulic binder, which is the basis of the waterproofing material, occurs; its deficiency is formed; and the maximum degree of hydration may decrease. Important factors influencing the adhesion of a waterproofing material are the method of applying the waterproofing coating and the curing conditions.

In the early stages of hardening, the formation of a tight and durable contact between the base concrete and the material of the waterproofing coating based on a binder hydraulic hardening and a polymeric modifier is due to the formation of bonds of various nature: ionic and valence (value (2–10) $\times$ $10^5$ J/mol), hydrogen ((0.1–0.3) $\times$ $10^5$ J/mol), as well as molecular bonds of (0.1–0.3) $\times$ $10^5$ J/mol [44,45].

At the stage of applying a waterproofing coating to the surface of concrete products and in the early stages of hardening, the adhesive contact of the cement particles of the waterproofing coating with the surface of the base concrete is due to electrostatic forces and capillary interaction forces. In the initial period, on the contact surface (the transition zone whose thickness is approximately equal to 1.3 $\times$ $10^{-10}$ m) of the base concrete and waterproofing, capillary interaction forces prevail. With the implementation of chemical reactions, absorption of moisture by the concrete surface and evaporation from the outer surface, the water content in the transition zone decreases and the forces of electrostatic and covalent interaction become predominant [46,47].

The assessment of the capillary component influence of the adhesive interaction of a separate cement particle of the waterproofing layer with the surface of the base concrete was carried out using the model. The shape of the mineral particle is assumed to be spherical. The scheme of interaction of a spherical mineral particle with a flat base surface through a liquid phase layer of thickness is shown in Figure 7.

The following designations were accepted: θ1is the wetting angle of the cement particle; θ2 is the wetting angle of the cement particle; r is the radius of the cement particle; ρ1 is the first main radius of curvature of the liquid cuff at its arbitrary point, located in the plane of the sheet; ρ2 is the second main radius of curvature of the liquid cuff at the same point, located in the plane perpendicular to the sheet; Rc is the wetting radius of the concrete surface with a liquid cuff.

The capillary component of the adhesion of a mineral particle to a flat concrete surface (Figure 7) depends on the coefficient of surface tension of thin water films (σ, N/m), as well as capillary pressure (Pk, Pa), determined through the main radii of curvature of the liquid cuff (ρ1 and ρ2, m) and can be calculated from the formulas:

$$F_k = 2\pi R_c \sigma + \pi \rho_2^2 \cdot P_k \quad (7)$$

$$P_k = \sigma \left( \frac{1}{\rho_1} + \frac{1}{\rho_2} \right) \quad (8)$$

In Formula (7), the first term characterizes the capillary component of adhesion due to the surface tension of the liquid along the wetting perimeter with radius Rc. The second term characterizes the capillary component of adhesion due to capillary pressure on the

wetting spot. Determination of capillary pressure using Formula (8), and adhesion strength using Formula (7) allows obtaining approximate results.

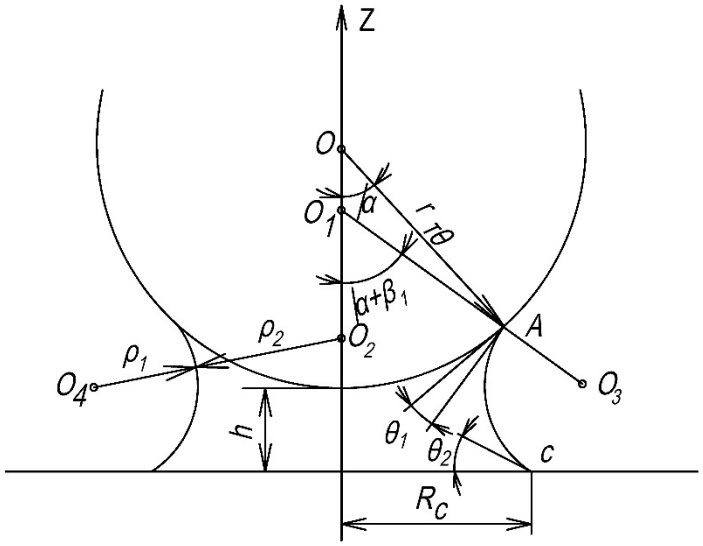


**Figure 7.** Scheme of the interaction of a mineral particle of a waterproofing material with a flat solid surface in the presence of a liquid phase between the surfaces of concrete and a waterproofing coating in the early stages of hardening.

More accurate calculated values can be obtained using the following relationship:

$$F_k = \frac{2\pi r\sigma}{k_1}, \text{ where } k_1 = \frac{1-\cos\alpha}{\cos\alpha + \cos\theta_2} \quad (9)$$

If we consider the surface of the base concrete to be completely wetted, then the value of the angle θ2 is greater than 0. In this case, the coefficient can be determined by the formula: $k_1 = tg^2\frac{\alpha}{2}$. The maximum value of Fk will be when the angle α is equal to zero or 90°. In this case, the capillary component of adhesion will be equal to: $F_k = 4\pi r\sigma$.

Taking into account the fact that σ = 72.5 × $10^{-3}$ N/m and r 2.5 × $10^{-5}$ m, we obtain: $F_k$ = 4 × 3.14 × 2.5 × $10^{-5}$ × 72.5 × $10^{-3}$ = 2.3 × $10^{-5}$ N. The maximum value of the capillary component of adhesion will be equal to:

$$A_k = \frac{F_k}{\pi r^2} = \frac{2.3 \cdot 10^{-5}}{3.14 \cdot 6.25 \cdot 10^{-10}} 11.6 \text{ kPa}$$

The total value of electrostatic (Ae) and capillary (Ak) adhesion at the time of application of the waterproofing coating will be:

$$A = Ae + Ak = 426.0 + 11.6 = 437.6 \text{ kPa}$$

As the cement-based waterproofing coating with acrylic additives hardens, the capillary component decreases, the electrostatic component remains constant. The basis of the adhesive strength of the waterproofing coating material to the base concrete will be performed by forces based on the chemical interaction of neoplasms in the hardening waterproofing coating and hydrosilicates of the base concrete.

The durability of the insulation system to the base material depends not only on the magnitude of the adhesive strength for the estimated hardening period, as well as the thickness of the layer and the conditions (aging) under which the waterproofing coating gains strength, but also on the reliability of adhesive contacts and changes (hardening or degradation) of properties over time. This property is largely determined by the presence and operating conditions of the adhesion layers.

In waterproofing coatings based on a hydraulic binder, the adhesive tensile strength is significantly reduced if no tie layer is used. As a binding layer, the same system was used, but more mobile and with a large flow of water. At the same time, in the solution with acrylic additives, the adhesive strength in the absence of a binder layer was 15–18% less than the strength achieved when using a binder layer. It was found that when the acrylic tie layer dried too much, the adhesive strength was less than if no tie layer was used at all.

The obtained results are used in the design of systems of cladding insulation with polymer–cement mixtures, and the optimization technique proposed in the article is applicable to solve any formulation and technological problems.

## 4. Conclusions

A promising way to protect structures, including structures buried in the ground, is external waterproofing systems based on a polymer-modified hydraulic binder. Compounds similar to them can be used in the repair of surfaces of structures made of concrete, reinforced concrete, as well as concrete reinforced with polymeric materials.

It has been established that after applying the waterproofing coating and in the early stages of hardening, electrostatic forces and forces of capillary interaction between the mineral particles of the waterproofing coating and the structural elements of the surface layers of the base concrete are the main factors in the formation of adhesive contact.

The conducted experiments allowed forming the basis for the methodology of selecting the composition and predicting the properties of waterproof protective and repair coatings, based on the use of nomograms. The optimum value of moisture content of the base surface (9.7–9.8%), allowed obtaining the maximum adhesion of the coating to the base, as well as to optimize the plasticizer consumption (0.38–0.39% by mass of water consumption.), allowed obtaining the coating with maximum adhesion to the base (up to 3.7–3.9 MPa) up to and maximum strength (35–36 MPa).

The adequacy of the obtained optimization solutions was checked at two levels. First, in the process of obtaining basic models (regression equations) in the Statistica program, the adequacy of the equations was checked by Fisher's criterion. Secondly, based on the results of analytical optimization, the second stage of verification was carried out. The conditions were set, by which the calculated values of factors were determined, and then an active experiment with obtaining full-scale samples was carried out. In this case, the amount of discrepancy between the calculated and experimental values of the results was evaluated.

**Author Contributions:** Conceptualization, A.Z. and S.B.; methodology, A.Z. and S.B.; software, A.Z.; validation, A.Z., S.B. and I.S.; formal analysis, I.S. and I.E.; investigation, S.B.; resources, S.B.; data curation, A.Z.; writing—original draft preparation, A.Z.; writing—review and editing, I.S. and I.E.; visualization, A.Z. and S.B.; supervision, I.S.; project administration, I.S.; funding acquisition, I.S. All authors have read and agreed to the published version of the manuscript.

**Funding:** The research was funded by the National Research Moscow State University of Civil Engineering (grant for fundamental and applied scientific research, project No. 41-392/130).

**Data Availability Statement:** The original contributions presented in the study are included in the article, further inquiries can be directed to the corresponding author/s.

**Conflicts of Interest:** The authors declare no conflicts of interest. The funders had no role in the design of the study; in the collection, analyses, or interpretation of data; in the writing of the manuscript; or in the decision to publish the results.

## References

1. Ali, R.T.-B. Waterproof breathable layers—A review. *Adv. Colloid Interface Sci.* **2019**, *268*, 114–135. [CrossRef] [PubMed]
2. Heinlein, U.; Thienel, K.-C.; Freimann, T. Pre-applied bonded waterproofing membranes: A review of the history and state-of-the-art in Europe and North America. *Constr. Build. Mater.* **2021**, *296*, 123751. [CrossRef]
3. Muhammad, N.Z.; Keyvanfar, A.; Abd, M.; Majid, Z.; Shafaghat, A.; Mirza, J. Waterproof performance of concrete: A critical review on implemented approaches. *Constr. Build. Mater.* **2015**, *101*, 80–90. [CrossRef]

4. Zhao, J.; Kong, X.X.; Wang, S.J.; Tang, L.; Ling, X.Z. Reducing the urban environment impact of joint leakage of underground prefabricated structures: Waterproof performance improvement of WSR-EPDM gasket. *Constr. Build. Mater.* **2023**, *393*, 132086. [CrossRef]
5. Gao, H.C.; Sun, W.D.; Wang, C.H.; Jing, M.L.; Yang, L.; Gao, H.; Zhao, R. Improving waterproof-breathable capability of degradable macroporous film/hemp hydroentangled nonwovens composite membranes by porous structure and surface wettability modification. *Colloids Surf. A Physicochem. Eng. Asp.* **2023**, *674*, 131963. [CrossRef]
6. You, X.L.; Wang, H.B.; He, J.X.; Qi, K. Fluorine-free and breathable polyethylene terephthalate/polydimethylsiloxane (PET/PDMS) fibrous membranes with robust waterproof property. *Compos. Commun.* **2023**, *40*, 101621. [CrossRef]
7. Chae, G.-T.; Yun, S.-T.; Choi, B.-Y.; Yu, S.-Y.; Jo, H.-Y.; Mayer, B.; Kim, Y.-J.; Lee, J.-Y. Hydrochemistry of urban groundwater, Seoul, Korea: The impact of subway tunnels on groundwater quality. *J. Contam. Hydrol.* **2008**, *101*, 42–52. [CrossRef] [PubMed]
8. Shang, J. Construction of Green Community Index System under the Background of Community Construction. *J. Build. Constr. Plan. Res.* **2019**, *7*, 115–125. [CrossRef]
9. Luo, J.D.; Shuai, M. The True Meaning of Social Management Innovation and the Practice of Community Construction: An Interview with Professor Luo Jiade, Ph.D. Supervisor of Tsinghua University. *Soc. Sci.* **2013**, *24*, 1–4.
10. Ha, H.; Taxen, C.; Williams, K.; Scully, J. Effects of selected water chemistry variables on copper pitting propagation in potable water. *Electrochim. Acta* **2011**, *56*, 6165–6183. [CrossRef]
11. Laaksoharju, M.; Gascoyne, M.; Gurban, I. Understanding groundwater chemistry using mixing models. *Appl. Geochem.* **2008**, *23*, 1921–1940. [CrossRef]
12. Wang, X.-W.; Yang, T.-L.; Xu, Y.-S.; Shen, S.-L. Evaluation of optimized depth of waterproof curtain to mitigate negative impacts during dewatering. *J. Hydrol.* **2019**, *577*, 123969.
13. Al-Qudah, O.; Woocay, A.; Walton, J. Identification of probable groundwater paths in the Amargosa Desert vicinity. *Appl. Geochem.* **2011**, *26*, 565–574. [CrossRef]
14. Banwart, S.A.; Gustafsson, E.; Laaksharju, M. Hydrological and reactive processes during rapid recharge to fracture zones: The Äspö large scale redox experiment. *Appl. Geochem.* **1999**, *14*, 873–892. [CrossRef]
15. Kværner, J.; Snilsberg, P. The Romeriksporten railway tunnel—Drainage effects on peatlands in the lake Northern Puttjern area. *Eng. Geol.* **2008**, *101*, 75–88. [CrossRef]
16. Mossmark, F.; Ericsson, L.O.; Norin, M.; Dahlström, L.-O. Hydrochemical changes caused by underground constructions—A case study of the Kattleberg rail tunnel. *Eng. Geol.* **2015**, *191*, 86–98. [CrossRef]
17. Huang, Y.; Jie, X.; Zhen, W. Research on Construction and Application of Evaluation Index System of Green Business Environment. In Proceedings of the Fifteenth International Conference on Management Science and Engineering Management. ICMSEM 2021; Lecture Notes on Data Engineering and Communications Technologies. Xu, J., García Márquez, F.P., Ali Hassan, M.H., Duca, G., Hajiyev, A., Altiparmak, F., Eds.; Springer: Cham, Switzerland, 2021; Volume 79. [CrossRef]
18. Mossmark, F.; Hultberg, H.; Ericsson, L.O. Effects of groundwater extraction from crystalline hard rock on water chemistry in an acid forested catchment at Gårdsjön, Sweden. *Appl. Geochem.* **2007**, *22*, 1157–1166. [CrossRef]
19. Talib, R.; Boyd, D.; Hayhow, S.; Ahmad, A.G.; Sulieman, M. Investigating Effective Waterproofing Materials in Preventing Roof Leaking; Initial Comparative Study: Malaysia, U.K. *Procedia Manuf.* **2015**, *2*, 419–427. [CrossRef]
20. Selník, P.; Nečadová, K.; Mohapl, M. Technology of Implementation of the Pitched Green Roof on the Testing Building EnviHut. *Procedia Eng.* **2016**, *161*, 1904–1909. [CrossRef]
21. Garcez, N.; Lopes, N.; De Brito, J.; Sá, G. Pathology, diagnosis and repair of pitched roofs with ceramic tiles: Statistical characterisation and lessons learned from inspections. *Constr. Build. Mater.* **2012**, *36*, 807–819. [CrossRef]
22. Gonçalves, M.; Silvestre, J.D.; De Brito, J.; Gomes, R. Environmental and economic comparison of the life cycle of waterproofing solutions for flat roofs. *J. Build. Eng.* **2019**, *24*, 100710. [CrossRef]
23. Lopes, J.G.; Correia, J.R.; Machado, M.X.B. Dimensional stability of waterproofing bituminous sheets used in low slope roofs. *Constr. Build. Mater.* **2011**, *25*, 3229–3235. [CrossRef]
24. Xue, X.; Yang, J.N.; Zhang, W.D.; Jiang, L.H.; Qu, J.; Xu, L.J.; Zhang, H.Q.; Song, J.R.; Zhang, R.P.; Li, Y.W.; et al. The study of an energy efficient cool white roof coating based on styrene acrylate copolymer and cement for waterproofing purpose—Part II: Mechanical and water impermeability properties. *Constr. Build. Mater.* **2015**, *96*, 666–672. [CrossRef]
25. Miyauchi, H.; Katou, N.; Tanaka, K. Force transfer mechanism on fastener section of mechanically anchored waterproofing membrane roofs under wind pressure during typhoons. *J. Wind. Eng. Ind. Aerod.* **2011**, *99*, 1174–1183. [CrossRef]
26. Silva, R.R.; Lopes, J.G.; Correia, J.R. The effect of wind suction on flat roofs: An experimental and analytical study of mechanically fastened waterproofing systems. *Constr. Build. Mater.* **2010**, *24*, 105–112. [CrossRef]
27. Garcez, N.; Lopes, N.; De Brito, J.; Silvestre, J. System of inspection, diagnosis and repair of external claddings of pitched roofs. *Constr. Build. Mater.* **2012**, *35*, 1034–1044. [CrossRef]
28. Aktas, Y.D.; Zhu, H.D.; Ayala, D.; Weeks, C. Impact of surface waterproofing on the performance of brick masonry through the moisture exposure life-cycle. *Build. Environ.* **2021**, *197*, 107844. [CrossRef]
29. Lin, Z.H.; Song, Y.H.; Chu, Y.N. An experimental study of the summer and winter thermal performance of an opaque ventilated facade in cold zone of China. *Build. Environ.* **2022**, *218*, 109108. [CrossRef]
30. Barbosa, M.T.G.; Rosse, V.J.; Laurindo, N.G. Thermography evaluation strategy proposal due moisture damage on building facades. *J. Build. Eng.* **2021**, *43*, 102555. [CrossRef]

31. Ter-Zakaryan, K.A.; Zhukov, A.D.; Bobrova, E.Y.; Bessonov, I.V.; Mednikova, E.A. Foam Polymers in Multifunctional Insulating Coatings. *Polymer* **2021**, *13*, 3698. [CrossRef]
32. Patent for Utility Model No. 199048 U1 Russian Federation, IPC E04B 1/76. Heat Insulating Multilayer Material: No. 2020115732: Applied for on 13.05.2020: Published on 11.08.2020/K. A. Ter-Zakaryan. 13.05.2020: Published 11.08.2020/ K. A. Ter-Zakaryan. Available online: https://elibrary.ru/item.asp?id=44647831 (accessed on 10 May 2024).
33. Erofeev, V.; Rodin, A.; Kalashnikov, V.; Erofeeva, I. Biocidal binders for the concretes of unerground constructions. *Proc. Eng.* **2016**, *165*, 1448–1454. [CrossRef]
34. Yusupova, A.A.; Akhmetova, R.T.; Treshchev, A.A.; Erofeev, V.T.; Bobrishev, A.A.; Shafigullin, L.N.; Lakhno, A.V. Production and investigation of properties of sulfide composite materials based on technogenic sulfur waste with titanium chloride as an activator. *Res. J. Pharm. Biol. Chem. Sci.* 2016; 7, 1614–1619.
35. Ter-Zakaryan, K.A.; Zhukov, A.D.; Bessonov, I.V.; Bobrova, E.Y.; Pshunov, T.A.; Dotkulov, K.T. Modified Polyethylene Foam for Critical Environments. *Polymer* **2022**, *14*, 4688. [CrossRef] [PubMed]
36. Shariatmadar, M.; Mahdavian, M.; Ramezanzadeh, B. Designing a novel waterproof thin-layer based on silicon-modified polyacrylate grafted 2D-graphene nanosheets for chloride-induced corrosion protection of rebar in concrete structures. *J. Taiwan Inst. Chem. Eng.* **2023**, *149*, 104987. [CrossRef]
37. Erofeev, V.; Dergunova, A.; Piksaikina, A.; Bogatov, A.; Kablov, E.; Startsev, O.; Matvievskiy, A. The effectiveness of materials different with regard to increasing the durability. *MATEC Web. Conf.* **2016**, *73*, 04021. [CrossRef]
38. Sokova, S.; Smirnova, N. Reliability assessment of waterproofing systems of buildings underground parts. *IOP Conf. Ser. Mat. Sci. Eng.* **2018**, *365*, 052028.
39. Pyataev, E.R.; Medvedev, A.A.; Poserenin, A.I.; Burtseva, M.A.; Mednikova, E.A.; Mukhametzyanov, V.M. Theoretical principles of creation of cellular concrete with the use of secondary raw materials and dispersed reinforcement. *MATEC Web. Conf.* **2018**, *251*, 01012. [CrossRef]
40. Erofeev, V.; Yausheva, L.; Bulgakov, A.; Bobryshev, A.; Shafigullin, L.; Afonin, V. Biological resistance of sulphur binder composites. *AIP Conf. Proc.* **2023**, *2612*, 040027. [CrossRef]
41. Travush, V.I.; Antoshkin, V.D.; Erofeev, V.T. The problem 7 forming triangular geometric line field. *MATEC Web. Conf.* **2016**, *86*, 01032. [CrossRef]
42. Shitikova, M.V.; Bobrova, E.Y.; Popov, I.I.; Zhukov, A.D. Energy Efficiency of Technical Thermal Insulation. In Proceedings of the International Multi-Conference on Industrial Engineering and Modern Technologies (FarEastCon), Vladivostok, Russia, 1–4 October 2019; pp. 1–4.
43. Zhukov, A.D.; Bessonov, I.V.; Popov, I.I.; Poudel, R.S. Energy-efficient Insulation Systems for Low-rise Buildings. *Russ. J. Build. Constr. Archit.* **2022**, *4*, 39–49. Available online: https://web.archive.org/web/20221122203810id_/https://vestnikvgasu.wmsite.ru/ftpgetfile.php?id=857 (accessed on 10 May 2023).
44. Lepeng, H.; Jianmin, H.; Ming, K.; Fengbin, Z.; Qiming, L. Capillary tension theory for predicting shrinkage of concrete restrained by reinforcement bar in early age. *Constr. Build. Mater.* **2019**, *210*, 63–70. [CrossRef]
45. Li, Y.; Li, J. Capillary tension theory for prediction of early autogenous shrinkage of self-consolidating concrete. *Constr. Build. Mater.* **2014**, *53*, 511–516. [CrossRef]
46. Garcia, A.; Dessev, T.; Guihard, L.; Chevallier, S.S.; Havet, M.; Le-Bail, A. Impact of external static electric field on surface tension of model solutions. *Innov. Food Sci. Emerg. Technol.* **2023**, *87*, 103406. [CrossRef]
47. Jamali, A.; Mendes, J.; Nagaratnam, B.; Lim, M. A new four stage model of capillary pressure in early age concrete: Insights from high capacity tensiometers. *Cem. Concr. Res.* **2022**, *161*, 106955. [CrossRef]